J. Fluid Mech. (1988), *vol.* 195, *pp.* 57–76
Printed in Great Britain

The evolution of cyclonic disturbances and lee waves over a topography in a rapidly rotating stratified flow

By HAMID T. HEFAZI† AND H. K. CHENG‡

† Department of Mechanical Engineering, California State University, Long Beach, CA 90840, USA

‡ Department of Aerospace Engineering, University of Southern California, Los Angeles, CA 90089, USA

(Received 22 August 1986 and in revised form 6 August 1987)

The temporal evolution of the flow patterns about a shallow bottom topography in a deep, rapidly rotating, stratified flow is studied on the basis of an inviscid Boussinesq model. The initial boundary-value problem, linearized for a thin three-dimensional obstacle, is solved for an impulsively started flow. The indicial response obtained reveals a window for the horizontal wavenumber spectra of the obstacle geometry. Only the portion of spectra within this window, which is shut at the start and widens linearly with increasing time, contributes to the solution. Thus, only the relatively large-scale, cyclonic feature associated with the wavenumber origin can dominate the flow in the early period, while the more familiar inertial wave system emerges much later.

Examples of solutions computed via an FFT algorithm confirm that, except in the two opposite limits for the zero and infinite stratification, the cyclonic disturbance and inertial waves coexist, but a solitary pressure hill associated with the cyclonic disturbance remains dominant throughout most evolution stages. For a sufficiently strong stratification, the solution to the linear pressure equation suggests the emergence of a secondary eddy in the lee; its significance and validity are discussed.

1. Introduction

The study of a rotating stratified flow about an obstacle is essential to an understanding of the dynamics of oceans and atmosphere. Disturbances generated by topographical features, in the presence of combined Coriolis and stratification effects, can produce far-reaching influences on the flow and wave patterns.

A familiar feature of deep, rotating fluids, which has been studied by many investigators, is the presence of the far-field inertial waves. A number of these studies focus on the rapidly rotating, homogeneous case in which the Rossby number R, defined as $R = u_c/\Omega_c L$, is small and an internal Froude number is infinite. Here u_c and L are characteristic velocity and horizontal length-scales of the flow and Ω_c is angular velocity of the undisturbed rotating fluid. The far-field features associated with the transverse uniform motion of an obstacle have been studied by Lighthill (1967, 1978), using the group-velocity concept. Motivated by the suggestion of a 'tilted Taylor column' (Hide, Ibbetson & Lighthill 1968), Cheng (1977) and Cheng & Johnson (1982) analysed the problem in an infinitely deep, rapidly rotating container as a boundary-value problem.

Redekopp (1975) studied the wave patterns generated by steady as well as oscillatory forcing disturbances travelling horizontally at a uniform speed in a rotating, linearly stratified fluid, employing the group-velocity approach. A tilting angle of the inertial-wave caustic is found, which is proportional to the Brunt–Väisälä frequency. It is also found that in an oscillatory case wave crests can appear upstream of the travelling disturbance.

The hydrostatic-balance approximation has been extremely useful in geophysical contexts and is justified in a certain limited domain of a highly stratified rotating flow, to be brought out below. Studies of Hogg (1973) within this domain reveal the existence of a form of an extended Taylor column in the sense suggested earlier by Hide (1971) and Ingersoll (1969), as indicated by the closed streamlines above the topography. Rapidly rotating fluids under hydrostatic balance have also been studied with comparable models by Huppert (1975), Buzzi & Tibaldi (1977), Hogg (1980), Smith (1979*a*, *b*, *c*) and Pierrehumbert (1987). The equations governing the pressure disturbance in these works reduce to the Laplace equation, which does not admit inertial waves.

From the viewpoint of a rational understanding of the geophysical fluid dynamic concepts for low Rossby number, a more explicit knowledge of the transition from the inertial-wave domain (corresponding to a vanishing stratification) to the hydrostatic-balance domain (corresponding to a strong stratification) is highly desirable. Apart from the need of a theoretical framework with which laboratory experiments at intermediate stratification levels can be compared, the interesting results based on the group-velocity concept (Redekopp 1975) for an arbitrary stratification requires further analysis in order to reconcile it with results of Hogg (1973) and others obtained for the hydrostatic-balance domain. Specifically, the group-velocity analysis would yield a far field in the strongly stratified case not in accord with Hogg's solution, which features an extended Taylor column, suggesting that the far-field analysis by the group-velocity method may not be complete. Motivated by these needs Cheng, Hefazi & Brown (1984) extended Cheng's (1977) formulation to a Boussinesq fluid, which provides a basis for the study of transition between the homogeneous and the highly stratified limits of the rotating fluids over shallow three-dimensional topographies. It turns out (Cheng *et al.* 1984) that the discrepancy results from a need for an elementary, but critical, modification to the group-velocity approach (and the related stationary-phase method) to account for the contribution of the long waves near the origin of the wavenumber spectrum, which is a singularity of the phase in this case. The treatment leads to an additional disturbance feature in the far field, completely distinct from the inertial waves which have a much shorter lengthscale. Characteristic of this new feature is a symmetrically distributed pressure hill (or a pressure depression if the topography has a negative displacement volume) far above the topography which coexists with the familiar lee waves.

Following the nomenclature of meteorology, such a perturbation with a hill-like pressure rise will be referred to as an *anticyclonic disturbance*. Note that it produces anticyclonic circulation (clockwise in the northern hemisphere) in a reference frame fixed to the undisturbed, rapidly rotating fluid. Likewise, the disturbance with a pressure depression is *cyclonic*. Following Cheng *et al.* (1984), we shall use the descriptive 'cyclonic' for this type of disturbance whenever the distinction between the cyclonic and anticyclonic disturbances is unnecessary. At this point we may mention that the cyclonic disturbance coexisting with the inertial waves could have been apparent from the stationary two-dimensional ridge solutions by Queney (1948)

and also by Smith (1979*a*), which do not assume hydrostatic balance, nor a low Rossby number. However, the cyclonic nature of the circulation is not so evident therein, since the infinite ridge does not permit eddy motion in a horizontal plane (for any reference frame). Of great relevance to the topic areas are studies of 'Lee Cyclogenesis' reviewed by Smith (1979*c*) and by Pierrehumbert (1987); the analytical works examined therein are concerned mostly with steady-state, ridge-type solutions and do not address directly the evolution process of cyclones. (Instead of the production process or the origin of a cyclone, as the word 'genesis' would literally imply, the 'cyclogenesis' in Smith's and Pierrehumbert's reviews are defined as a fall in pressure greater than a certain magnitude.) Certain relations of the present work to those in Smith and Pierrehumbert will be noted in the text below.

The major question unanswered in Cheng *et al.* (1984, referred to hereinafter as I) is whether this steady-state description is realizable at the end of an evolutionary process ($t \to \infty$) irrespective of the initial state. Of interest also is the manner in which the inertial waves and cyclonic disturbance emerge during the evolution. To answer these questions, the unsteady problem of an impulsively started flow, to be referred to as the *indicial* problem, will be solved in this paper. In a development parallel to the present study, Brown & Cheng (1987) studied the effect of a sinusoidally pulsating topography on a stratified rapidly rotating flow. Their analysis confirms the coexistence of the oscillatory cyclonic and lee-wave patterns at all pulsating frequencies and all degrees of stratification, except in the homogeneous case.

It was not altogether clear if the cyclonic and lee-wave patterns can both become prominent at an early stage of an indicial or other non-periodic motion. The indicial solution obtained below will show explicitly that, owing to the limited size of a wavenumber window, the radius of which is a linear function of time, the densely packed lee waves pertaining to the high wavenumbers emerge only long after the large-scale cyclonic component appears.

The results may shed light on a possible route to the anticyclone generation above topography, and the emergence of cyclonic eddies in the lee, at least in the laboratory studies where inertial waves and cylonic disturbance can coexist. The phenomena may have relevance to transient eddy generation in the ocean, and has received considerable attention, even though there is a distinct difference with regard to the ratio of the depth to the horizontal scales. For example, Huppert & Bryan (1975) examined the interaction between temporally varying currents developing above a bottom topography of the ocean by a numerical integration of a nonlinear, time-dependent model problem. Their results indicate that during the evolution, a region of high pressure with anticyclonic vorticity develops rather rapidly over an isolated seamount. In the meantime, a region of low pressure with cyclonic vorticity is induced, which for sufficiently strong oncoming flows is convected downstream. An anticyclone above an isolated ground topography with accompanying cyclonic eddies in the lee has been reported in many observational and computational studies in the geophysical context (Richardson 1980; Chung, Hage & Reinelt 1976; Manabe & Terpstra 1974; Egger 1974; Buzzi & Tibaldi 1977; Smith 1979*c*).

Our analytic solution of the initial boundary-value problem will provide a description of the temporal evolution of the flow within a linearized framework and indicate that the aforementioned anticyclonic disturbance builds up rapidly from an early period and persist throughout subsequent stages of the evolution. This, along with the later appearance and intensification of inertial waves in the lee, may lead to an emerging pattern consisting of small-scale secondary eddies with directions of rotation opposite to that of the main one, depending on the degree of stratification

and the topography. These and other dynamical features will be brought out in the following development and by the examples analysed. A significant feature brought out by the analyses in I and Brown & Cheng (1987) deserving amplification is the explicit dependence of the cyclonic disturbance in the far field on the topographical (displacement) volume and the latter's significant influence on the near field. Examples illustrating this feature will also be shown, which should be of interest to the design of laboratory experiments.

In §2, the assumptions and framework are briefly stated, the basic scales and parameters are defined, and the relevant equations constituting the initial boundary-value problem for a shallow topography are derived. In §3 the indicial problem in which the uniform relative motion is impulsively started is formulated, and the solutions for two- and three-dimensional cases are obtained; the frequency response and the response to other more general obstacle (relative) motions are delineated via the Duhamel integral. The evolutionary process of the cyclonic and lee-wave features in the impulsively started flow is studied in §4 where examples computed via an FFT algorithm are presented. Certain analytical details omitted here are more fully presented in Hefazi (1985).

2. Model, assumptions, coordinates and governing equations

The geometry of the problem to be considered is illustrated in figure 1 (*a*, *b*) and is similar to that of I, except for the allowance of a time dependence. The large container of depth H is filled with a stably stratified inviscid fluid which initially is in a state of rigid-body rotation about its axis with a constant angular velocity Ω_c. The system of coordinates (x^*, y^*, z^*) is fixed to the horizontal base of the container, thus rotating with the undisturbed fluid. The components of the perturbation velocities corresponding to the x^*, y^*, z^* directions are denoted by u^*, v^*, w^*. An alternative system of coordinates (x'^*, y^*, z^*), where $x'^* = x^* - u_c t^*$, is attached to the obstacle or bottom topography of typical length of $2L$, moving slowly in the horizontal plane with a typical velocity u_c. A Boussinesq fluid with a linear density variation of the undisturbed fluid is assumed, i.e.

$$\frac{\rho_e^* - \rho_0^*}{\rho_0^*} = -\epsilon \frac{Z^*}{H}, \tag{2.1}$$

where ρ_e^* is the equilibrium density, ρ_0^* is the density at the base $z = 0$, and ϵ is a positive constant. The stratification parameter is

$$\theta = g \frac{\epsilon}{H} \frac{L^2}{u_c^2}, \tag{2.2}$$

which is simply the inverse square of a Froude number U_c/NL (Yih 1965, 1980), noting that $N = (g\epsilon/H)^{\frac{1}{2}}$ is the Brunt–Väisälä frequency. The quantity $\Theta = RH/L$ is the product of Rossby number and the aspect ratio of the container. In the interest of analysing the region far from the moving obstacle, the present study considers an unbounded Θ, corresponding to a very deep container which is also assumed to have horizontal dimensions much larger than the obstacle so that the effects of the sidewalls are ignored.

Let τ denote the non-dimensional thickness ratio of the topography and

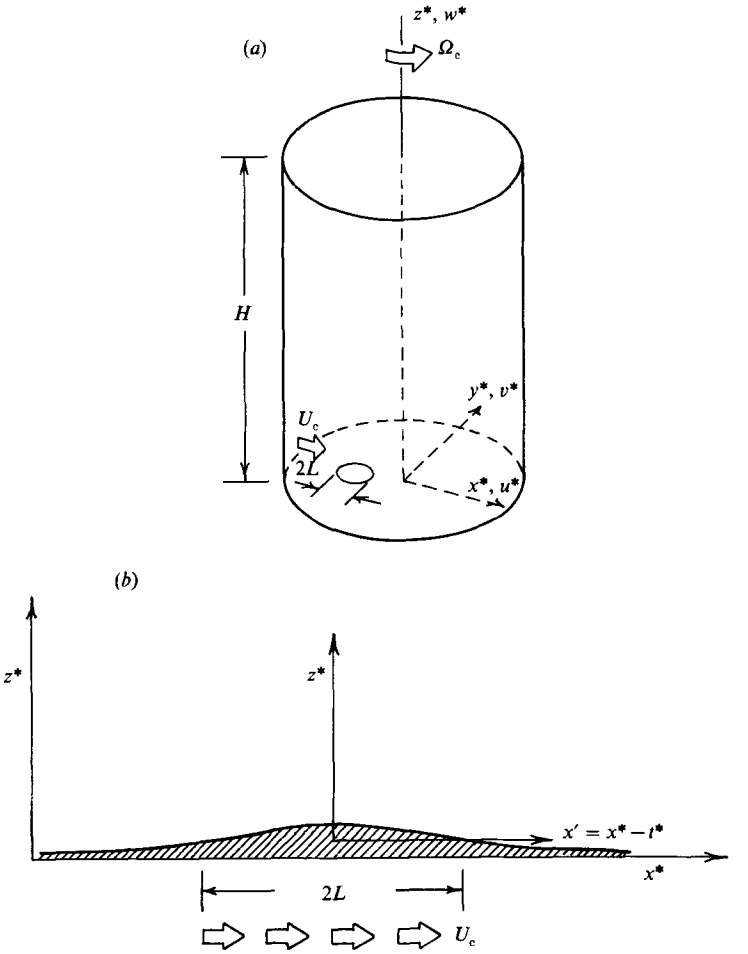

FIGURE 1. (*a*) Illustration of coordinates and notation used in the analysis. (*b*) The container-fixed, body-fixed coordinates and the profile of the three-dimensional topography considered in §4.2.

$R = u_c/\Omega_c L$ be the Rossby number. Following I, we define a set of normalized variables, t, x, y, z; u, v, w, p and ρ from

$$t^* = tL/u_c, \quad x^*, y^*, z^* = L(x, y, 2\hat{z}/R), \quad u^*, v^*, w^* = u_c(u, v, w), \qquad (2.3a, b, c)$$

$$p^* - p_e^* = p\tau\rho\Omega_c u_c L, \quad \rho^* - \rho_e^* = \rho\tau\epsilon\rho_0 L/H, \qquad (2.3d, e)$$

where p^* and ρ^* are the pressure and density in their original scales, and the subscript e refers to the local equilibrium value. The bottom topography is given by

$$z = \tau Z_w(x - t, y, t), \qquad (2.3f)$$

where $|Z_w|$ is of unit order.

For a shallow topography in a rapidly rotating fluid ($R \ll 1$, $\tau \ll 1$), the equations of motion, following I, can be simplified to a linearized, inertial-baroclinic system

$$-2v + \frac{\partial p}{\partial x} = 0, \quad 2u + \frac{\partial p}{\partial y} = 0, \qquad (2.4a, b)$$

$$\frac{1}{2}\frac{\partial p}{\partial \hat{z}} + \frac{\partial w}{\partial t} + \theta p = 0, \quad \frac{\partial w}{\partial \hat{z}} - \frac{\partial}{\partial t}\left(\frac{\partial v}{\partial x} - \frac{\partial u}{\partial y}\right) = 0, \quad \frac{\partial \rho}{\partial t} - w = 0, \qquad (2.4c\text{–}e)$$

with the impermeable boundary condition

$$w = \frac{\partial}{\partial t} Z_w(x\text{-}t, y, t) \quad \text{on } \hat{z} = 0. \tag{2.5}$$

In the coordinate system $(x', y, \hat{z})$, fixed to the obstacle, where $x' = x\text{-}t$, (2.4) can be combined to yield a single equation in terms of normalized perturbation pressure ψ

$$\left(\frac{\partial}{\partial t} - \frac{\partial}{\partial x'}\right)\left\{\frac{\partial^2}{\partial \hat{z}^2} + \left[\left(\frac{\partial}{\partial t} - \frac{\partial}{\partial x'}\right)^2 + \theta\right]\nabla_1^2 \psi\right\} = 0, \tag{2.6a}$$

where

$$\psi = -\tfrac{1}{2}p, \quad \nabla_1^2 = \frac{\partial^2}{\partial x'^2} + \frac{\partial^2}{\partial y^2},$$

with the boundary condition (2.5) replaced by

$$\left(\frac{\partial}{\partial t} - \frac{\partial}{\partial x'}\right)\left\{\frac{\partial \psi}{\partial \hat{z}} - \left[\left(\frac{\partial}{\partial t} - \frac{\partial}{\partial x'}\right)^2 + \theta\right] Z_w(x', y, t)\right\} = 0. \tag{2.6b}$$

Assuming quiescent uniform, initial and upstream states ($u = v = w = \rho = 0$), the advective operator outside the curly bracket in (2.6*a*, *b*) can be omitted. The assumptions of vanishing disturbances as $(x'^2 + y^2 + \hat{z}^2)^{\frac{1}{2}} \to \infty$ and the condition that in the steady state there are only outgoing waves in the far field (radiation condition) will also be invoked.

While (2.6*a*, *b*) are linearized for a shallow topography and a finite stratification ($\tau \ll 1$, $\theta = O(1)$), they also describe the more strongly stratified geostrophic flow in the domain $\tau\theta^{\frac{1}{2}} \neq 0$, $\tau \ll 1$ (cf. I). In this case, the system is generally nonlinear, but the equation governing ψ is given by a limiting form of (2.6) in which terms associated with $\partial/\partial t$ and $\partial/\partial x'$ are relatively small and can be deleted. In this manner the strongly stratified rapidly rotating case of Hogg (1973) and others is recovered. The linear system (2.6) may therefore be used as a model to study the transition from the homogeneous limit to the highly stratified domain of non-vanishing $\tau\theta^{\frac{1}{2}}$, as in §6.3 of I.

It is essential to point out that the system (2.4*a–e*) is derived from a Boussinesq version of the inviscid model by deleting terms of order R relative to those retained in each of the (full) equations. Equation (2.4*d*) involving $\partial w/\partial \hat{z}$ and the time derivative of the horizontal vorticity is derived from the continuity equation combined with the two horizontal momentum equations, but requires a knowledge of the higher-order inertial contributions omitted from (2.4*a*, *b*)†. Therefore (2.4*d*) as such could not have been deduced directly from the relation between velocity and pressure of (2.4*a*, *b*). The simplification of the horizontal momentum equations for a small R, leading to (2.4*a*, *b*) may be referred to as geostrophic or quasi- (nearly) geostrophic approximation following the convention used in many texts (e.g. Batchelor 1967, p. 572; Pedlosky 1979, p. 50). In some works on rotating stratified flows in a meteorological context, the hydrostatic-balance approximation (for the perturbation field) is implicit, and, in fact, is considered synonymous with the assumption of a geostrophic approximation (e.g. Pierrehumbert 1987). Following traditional usage, however, we consider the two approximations as being distinct; thus, the $\partial w/\partial t$ term in (2.4*c*) is retained, which would have been absent in a hydrostatic-balance approximation but is crucial for the recovery of the inertial

† The procedure was used in deriving the basic equations in Cheng (1977) for the homogeneous case.

waves. The hydrostatic-balance approximation can nevertheless be recovered in a certain limit corresponding to a sufficiently high θ (cf. I).

In passing, we note that a parameter encountered often in the meteorological application is $S = (L_D/L)^2$, where $L_D = (-gd(\ln\rho)/dz)^{\frac{1}{2}}\, H/\Omega_c$ is a Rossby deformation radius and H the height of fluid. S may be related to θ and a reduced height $\Theta = RH/L$ as

$$S = \theta\Theta^2 = \Theta_s^2, \tag{2.7}$$

which may therefore be recognized as another reduced vertical-to-horizontal scale ratio. For the problem of infinite depth considered below, S is infinite, whereas in most 'synoptic-scale' examples in meteorological studies $S = O(1)$.

3. The initial boundary-value problem

In this section, the initial boundary-value problem of (2.6) corresponding to an obstacle accelerated impulsively from rest to a uniform speed is formulated, i.e. we consider the flow response to an indicial obstacle motion

$$Z_w(x', y, t) = Z_w(x', y)\, 1(t),$$

where $1(t)$ is the unit step function

$$1(t) = \begin{cases} 1, & t > 0, \\ 0, & t \leqslant 0. \end{cases}$$

The response of the flow system to other more general obstacle motions, including an oscillatory heaving motion, can be obtained from this indicial solution by a convolution via the Duhamel's integral. One such case will be discussed in §3.4.

The impermeable boundary condition (2.5) for the present case becomes

$$w = \left(\frac{\partial}{\partial t} - \frac{\partial}{\partial x'}\right) Z_w(x', y)\, 1(t) = Z_w(x', y)\, \delta(t) - \frac{\partial}{\partial x'} Z_w(x', y)\, 1(t),$$

which may be interpreted as that due to a sudden rise of a current. Imposing this boundary condition after $t = 0^+$ would result in

$$w = -\frac{\partial}{\partial x'} Z_w(x', y)\, 1(t),$$

which in terms of the normalized perturbation pressure, via (2.4), would give for $t > 0^+$

$$\frac{\partial}{\partial \hat{z}} = \left[-\frac{\partial}{\partial x'}\left(\frac{\partial}{\partial t} - \frac{\partial}{\partial x'}\right) + \theta\right] Z_w(x', y)\, 1(t). \tag{3.1}$$

Equations (2.6*a*), with the time derivative outside the bracket omitted, and (3.1) along with the assumptions of an undisturbed initial state, and vanishing disturbances in the far field for $t \neq \infty$, complete the formulation of this initial boundary-value problem.

3.1. *The three-dimensional solution*

Let $F(\omega, \sigma)$ be the double Fourier transform of the surface elevation $\hat{z} = Z_w(x', y)$, and let $\bar{\psi}(x', y, z, s)$ denote the Laplace transform of the solution $\psi(x', y, z, t)$ with respect to t, i.e.

$$F(\omega, \sigma) = \frac{1}{(2\pi)^2} \int_{-\infty}^{\infty} \int_{-\infty}^{\infty} Z_w(x', y)\, \mathrm{e}^{-\mathrm{i}(\omega x' + \sigma y)}\, \mathrm{d}x' \mathrm{d}y,$$

$$\bar{\psi}(x', y, \hat{z}, s) = \int_0^{\infty} \psi(x, y, \hat{z}, t)\, \mathrm{e}^{-st}\, \mathrm{d}t.$$

We point out that the assumption of an undisturbed initial state requires that $u = v = w = p = 0$ at $t = 0^+$, which also implies through (2.4) a zero initial time derivative for the velocity, density, and the horizontal vorticity $(\partial^2/\partial x'^2 + \partial^2/\partial y^2)\psi$. The latter condition is needed to obtain the Laplace transform of the solution to (2.6), since the equation is second order in t. The function ψ satisfying the boundary condition may then be written as (cf. Hefazi 1985)

$$\bar{\psi}(x', y, z, s) = \int_{-\infty}^{\infty}\int_{-\infty}^{\infty} \{h(\omega, \sigma, s)\, \mathrm{e}^{-b[(s-\mathrm{i}\omega)^2+\theta]^{\frac{1}{2}}}\} \mathrm{e}^{\mathrm{i}(\omega x' + \sigma y)}\, \mathrm{d}\omega\, \mathrm{d}\sigma \tag{3.2a}$$

where
$$b = \hat{z}\,(\omega^2 + \sigma^2)^{\frac{1}{2}} > 0$$

and
$$h(\omega, \sigma, s) = \frac{F(\omega, \sigma)}{(2\pi)^2\,(\omega^2+\sigma^2)^{\frac{1}{2}}} \left\{\frac{\mathrm{i}\omega(s-\mathrm{i}\omega)-\theta}{s\,[(s-\mathrm{i}\omega)^2+\theta]^{\frac{1}{2}}}\right\}. \tag{3.2b}$$

The solution now can be expressed as

$$\psi = \frac{1}{(2\pi)^2}\int_{-\infty}^{\infty}\int_{-\infty}^{\infty} \frac{F(\omega, \sigma)}{(\omega^2+\sigma^2)^{\frac{1}{2}}}\, \mathscr{L}^{-1}\left(\frac{\mathrm{i}\omega(s-\mathrm{i}\omega)-\theta}{s[(s-\mathrm{i}\omega)^2+\theta]^{\frac{1}{2}}}\, \mathrm{e}^{-b[(s-\mathrm{i}\omega)^2+\theta]^{\frac{1}{2}}}\right) \mathrm{e}^{-\mathrm{i}(\omega x' + \sigma y)}\, \mathrm{d}\omega\, \mathrm{d}\sigma, \tag{3.3}$$

where $\mathscr{L}^{-1}$ is the inverse Laplace transform operator. In passing we may mention that (3.2*a*, *b*) in the limit $s \to 0$ yields

$$\lim_{s\to 0} s\bar{\psi} = \int_{-\infty}^{\infty}\int_{-\infty}^{\infty} \left\{\frac{-\mathrm{i}F(\omega, \sigma)}{(2\pi)^2\,(\omega^2+\sigma^2)^{\frac{1}{2}}}(\omega^2-\theta)^{\frac{1}{2}}\, \mathrm{e}^{-\mathrm{i}b(\omega^2-\theta)^{\frac{1}{2}}}\right\} \mathrm{e}^{-\mathrm{i}(\omega x' + \sigma y)}\, \mathrm{d}\omega\, \mathrm{d}\sigma \tag{3.4}$$

from which we recover the steady-state solution of I after applying the radiation condition by properly defining (cf. I).

$$(\omega^2-\theta)^{\frac{1}{2}} = \mathrm{i}\ \mathrm{sgn}\,(\omega+\theta)\,(\omega^2-\theta)^{\frac{1}{2}}, \tag{3.5}$$

where
$$\mathrm{sgn}\,(\alpha) = \begin{cases} +1, & a > 0, \\ -1, & a < 0. \end{cases}$$

When $s = \mathrm{i}\Omega$ is purely imaginary, the radiation condition requires

$$[(\omega-\Omega)^2-\theta]^{\frac{1}{2}} = \left.\begin{cases} +\,|\,(\omega-\Omega)^2-\theta\,|^{\frac{1}{2}} & \text{if } \omega-\Omega > \theta^{\frac{1}{2}} \\ -\,|\,(\omega-\Omega)^2-\theta\,|^{\frac{1}{2}} & \text{if } \omega-\Omega < -\theta^{\frac{1}{2}} \\ \mathrm{i}\,|\,(\omega-\Omega)^2-\theta\,|^{\frac{1}{2}} & \text{if } |\,\omega-\Omega\,| < \theta^{\frac{1}{2}} \end{cases}\right\} \tag{3.6}$$

This limit corresponds to the solution of Brown & Cheng (1987) for the steady oscillatory motion of the obstacle, which will be recovered in a later section.

The key to the explicit solution obtained in this section lies in the inversion of the Laplace transform in (3.3) which is given by

$$\mathscr{L}^{-1}(\ ) = [\mathrm{i}\omega\, \mathrm{e}^{\mathrm{i}\omega t} f(t) + (\omega^2-\theta)\int_b^t \mathrm{e}^{\mathrm{i}\omega p} f(p)\, \mathrm{d}p]\, \Pi(t-b). \tag{3.7}$$

Here $\Pi(t-b)$ is a circular unit step function defined as

$$\Pi(t-b) = \begin{cases} 1, & t > b, \\ 0, & t < b, \end{cases} \qquad b = \hat{z}\,(\omega^2+\sigma^2)^{\frac{1}{2}},$$

and $f(t) = J_0[\theta(t^2-b^2)]^{\frac{1}{2}}$, where J_0 is the Bessel function of first kind and zeroth order and the definition of b is unchanged. Essential to this derivation is the proper choice

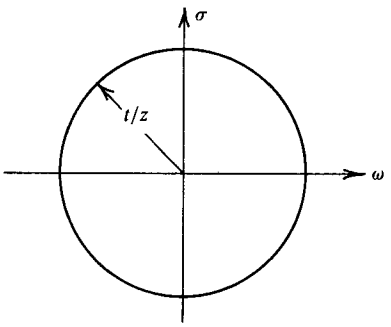

FIGURE 2. Illustration of the circular wavenumber window.

of the branch cut and the definition of the function $[(s-\mathrm{i}\omega)^2+\theta]^{\frac{1}{2}}$ in the complex-s plane. This along with other details of the above derivation are described in the Appendix. A fuller presentation is given in Hefazi (1985).

The solution (3.3), (3.7) exists in the Riemann sense and can be shown to directly satisfy the governing equations and the required boundary condition and therefore is indeed the indicial response in question. A solution similar to (3.3), (3.7) may be obtained for the vertical velocity component w, recalling that the equation governing w is identical to (2.6a) and the proper boundary condition is given by (2.5).

The appearance of the circular step function Π in (3.7) signifies that, at any given time, only the wavenumbers inside a circular window with the radius t/z in the (ω, σ)-plane contribute to the solution. This is illustrated in figure 2. It can readily be inferred from this window that the large-scale cyclonic (or anticyclonic) disturbance, rather quickly asserts itself in the early stages of the evolutionary process, since the wavenumbers in the vicinity of $\omega = \sigma = 0$ are the first to appear in the window. This feature will be substantiated by numerical calculations in a later section.

3.2. *The two-dimensional solution*

The solution (3.3) for a two-dimensional ridge-type topography $Z_w(x')$ reduces formally to

$$\psi = \frac{1}{2\pi}\int_{-\infty}^{\infty} \frac{F(\omega)}{\omega}\,(\text{right-hand side of (3.7)})\,\mathrm{e}^{\mathrm{i}\omega x'}\,\mathrm{d}\omega \tag{3.8}$$

with (3.7) unchanged, except that the circular step function $\Pi(t-b)$ is replaced with the one-dimensional step function $1(t/\hat{z}-|\omega|)$. As in the steady-state solution considered in I, the formal integral (3.8) does not exist in the Riemann sense and should be defined over an indented contour. However, the horizontal velocity $\partial\psi/\partial x'$, can be readily calculated from (3.8) and ψ is recovered subsequently by quadrature as in I. It is also interesting to note that the spanwise component of an oblique (relative) wind has no effect on $\psi(x', t)$, for which u_c must be taken to be the normal component of the far-field wind velocity.

3.3. *The steady-state limit*

As $t \to \infty$, the function $\Pi(t-b)$ approaches unity, thus the wavenumber window is completely open. For a compact topography, the function $F(\omega, \sigma) \to 0$ as $\rho \equiv (\omega^2+\sigma^2)^{\frac{1}{2}} \to \infty$. Therefore, owing to the pressure of the factor $F(\omega, \sigma)/\rho$ in (3.3), only finite wavenumbers (finite ρ) contribute to the solution. For a finite $b \equiv \rho\hat{z}$, the

first part of (3.7), $J_0[\theta(t^2-b^2)]^{\frac{1}{2}}$, vanishes for $t \to \infty$. The second right-hand member of (3.7) may also be written as

$$I = (\omega^2-\theta)\int_b^\infty e^{i\omega p} J_0[\theta(p^2-b^2)]^{\frac{1}{2}}\,dp. \tag{3.9}$$

The integral (3.9) after a change of variable can be evaluated as

$$I = (\omega^2-\theta)\frac{e^{-b}(\theta-\omega^2)^{\frac{1}{2}}}{(\theta-\omega^2)^{\frac{1}{2}}}. \tag{3.10}$$

With $(\theta-\omega^2)^{\frac{1}{2}}$ given by (3.5), (3.10) recovers the steady-state solution of I.

In passing we note that the two-dimensional analysis of steady flow over mountains at low R by Pierrehumbert (1987) stipulates a hydrostatic balance, and for an infinite depth, this result can be recovered from I for the limit $\theta \to \infty$.

3.4. *From indicial response to frequency response*

As mentioned before, the response of the system (2.6) to other types of motions can be obtained from the indicial response. As an example, we can recover the solution obtained by Brown & Cheng (1987) for the steady oscillatory motion of the obstacle, i.e.

$$Z_w(x', y, t) = Z_w(x', y)\, e^{i\Omega t}$$

where Ω is the frequency of oscillation.

If ψ_f denotes the frequency response of the system, and ψ is the indicial solution (3.3), (3.7), Duhamel's integral gives

$$\psi_f = \psi(0)\,F(t) + \int_0^t F(\tau)\frac{\partial}{\partial t}[\omega(t-\tau)]\,d\tau,$$

where for simplicity only dependence of the functions on time is indicated. Furthermore, the initial condition $\psi(x', y, \hat{z}, 0) = 0$ will give

$$\psi_f = \int_0^t F(\tau)\frac{\partial}{\partial t}[\psi(t-\tau)]\,d\tau. \tag{3.11}$$

Substituting for ψ from (3.3), (3.7) in (3.11), using Leibnitz's rule to evaluate the time derivative, and reversing the order of integration with respect to τ and (ω, σ), (3.11) leads to a form which in the limit $t \to \infty$ is identifiable with the solution in Brown & Cheng (1987) where the far-field is analysed in detail and a number of novel far-field features are brought out. The present and Brown & Cheng's analysis are thus shown to be completely consistent and provide two complementary description of the unsteady flow patterns.

4. Computation

The solution (3.3), (3.7) and (3.8) can be viewed as the inversed Fourier transforms of functions of t and $\hat{z}$ and thus be evaluated via one- and two-dimensional fast Fourier transform (FFT) algorithms for any time t and altitude $\hat{z}$. Steady-state solutions have been studied in I and in Hefazi (1985) where examples with two- and three-dimensional cases considered therein, which illustrate most directly the effects of the cyclonic component on the horizontal flow pattern and the tendency towards developing *closed* streamlines. The unsteady analysis in the form of an indicial solution presented here will show how these cyclonic and other features emerge in time.

It should be pointed out again that a horizontal flow pattern with closed streamlines over a *shallow* topography is an anticipated feature in a rapidly rotating fluid with a stratification strong enough to maintain hydrostatic balance (Hogg, 1973). Even though the problem is not strictly linear, the governing equation in this particular limit ($\theta R^2 \neq \infty$) is recoverable from the linear system for ψ (2.6*a*, *b*) as $\theta \to \infty$, subject to error comparable with R and τ, according to I. Therefore, the closed streamlines appearing in the case $\theta = 5$ in I may not be taken as evidence for a solution breakdown. The question on relevance and validity of the result involving closed streamlines will be more specifically discussed in §4.2.

4.1. *Application of the FFT algorithm*

The two-dimensional FFT algorithm that is used in computing the three-dimensional solutions typically employs 512 uniform ω-divisions over the range of $|\omega| < 16\pi$, and 128 uniform divisions over the range of $|\sigma| < 4\pi$ with mesh spacing $\Delta\omega = \Delta\sigma = 2\pi/64$, which results in $\Delta X = \frac{1}{8}$ and $\Delta Y = \frac{1}{2}$, where X and Y are defined as $x'/\hat{z}$ and $y/\hat{z}$ respectively. The choice of these parameters is based upon the need for a sufficiently fine mesh in (ω, σ) to resolve the singularity $1/(\omega^2+\sigma^2)^{\frac{1}{2}}$ in the solution (3.3), (3.7) and yet maintain large enough upper limits on ω and σ with a fixed number of mesh points. The resulting mesh in X and Y is merely the location at which the solution is available and does not affect the truncation error. Discretization in ω and σ however could introduce errors as high as $(\Delta\omega + \Delta\sigma)$ in the FFT solution owing to the singularity, but detailed comparisons of asymptotic and FFT solutions (for the steady case) presented in I and Cheng & Johnson (1982) confirm the quality of computations within the ranges of parameters discussed here. The discontinuity in the integrand of (3.3), (3.7) due to the circular unit step function $\Pi(t-b)$ is also noteworthy. The integrand is defined as the mid-value at this discontinuity.

4.2. *The three-dimensional example*

The example presented here is for the smooth three-dimensional topography with $Z_w^*/L = \tau Z_w = \tau(1+x'^2+y^2)^{-2}$ for which $F(\omega, \sigma) = \pi\rho K_1(\rho)$, where $\rho = (\omega^2+\sigma^2)^{\frac{1}{2}}$ and K_1 is the Bessel function for the second kind of the first order. This is the same geometry considered in I.

As indicated earlier, the primary objective of this study is to understand the evolutionary process of the high (low)-pressure region above the topography as a distinct anticyclone (cyclone) disturbance resulting from the influence of the stratification on rapidly rotating fluid. Two levels of stratification will be considered, $\theta = 1$ and $\theta = 5$, which were the cases studied in I in great detail. Neither of these cases is close to the hydrostatic-balance domain, but it serves to illustrate how inertial waves may modify a strong cyclonic-disturbance field at different stages leading to the steady state. The evolution history for the case $\theta = 5$ and thickness ratio $\tau = 0.25$ is of particular interest, since horizontal streamline patterns computed from the steady-state solution show not only (anticyclonic) closed streamlines but the appearance of a (cyclonic) secondary eddy.

The bottom geometry is shown in figure 1(*b*) and can be qualified as a *thin* topography.

Figure 3(*a–e*) describes the evolution of the streamline patterns at a mid-altitude $\hat{z} = 0.5$ above the thin topography with a thickness ratio $\tau = \frac{1}{4}$ for $\theta = 5$. The streamlines are obtained as contours of constant stream function given by

$$\psi_{\text{total}} = -y + \tau\psi. \tag{4.1}$$

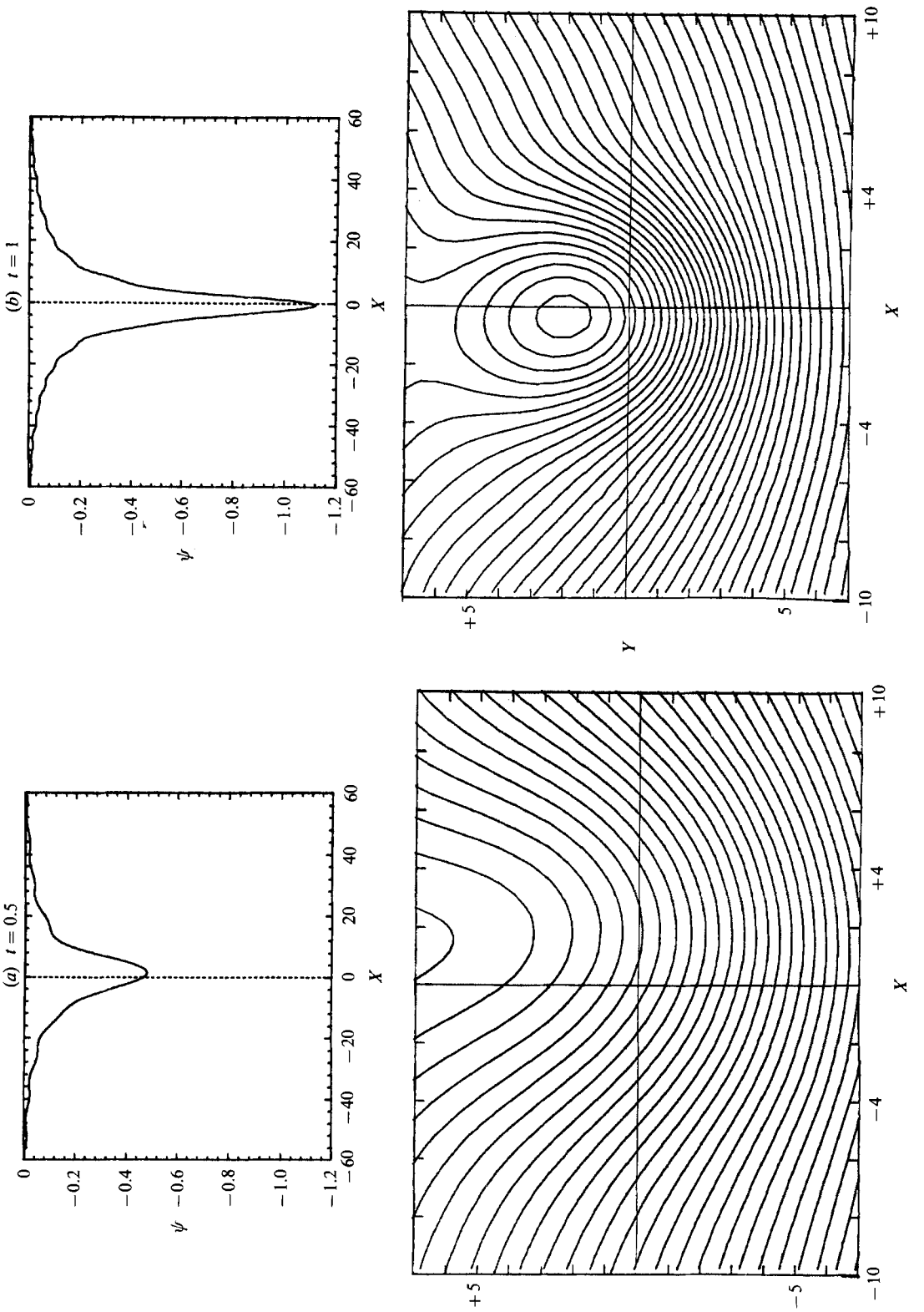
(a) t = 0.5
(b) t = 1
ψ
X
Y
0
−0.2
−0.4
−0.6
−0.8
−1.0
−1.2
−60
−40
−20
0
20
40
60
+5
−5
−10
+4
+10

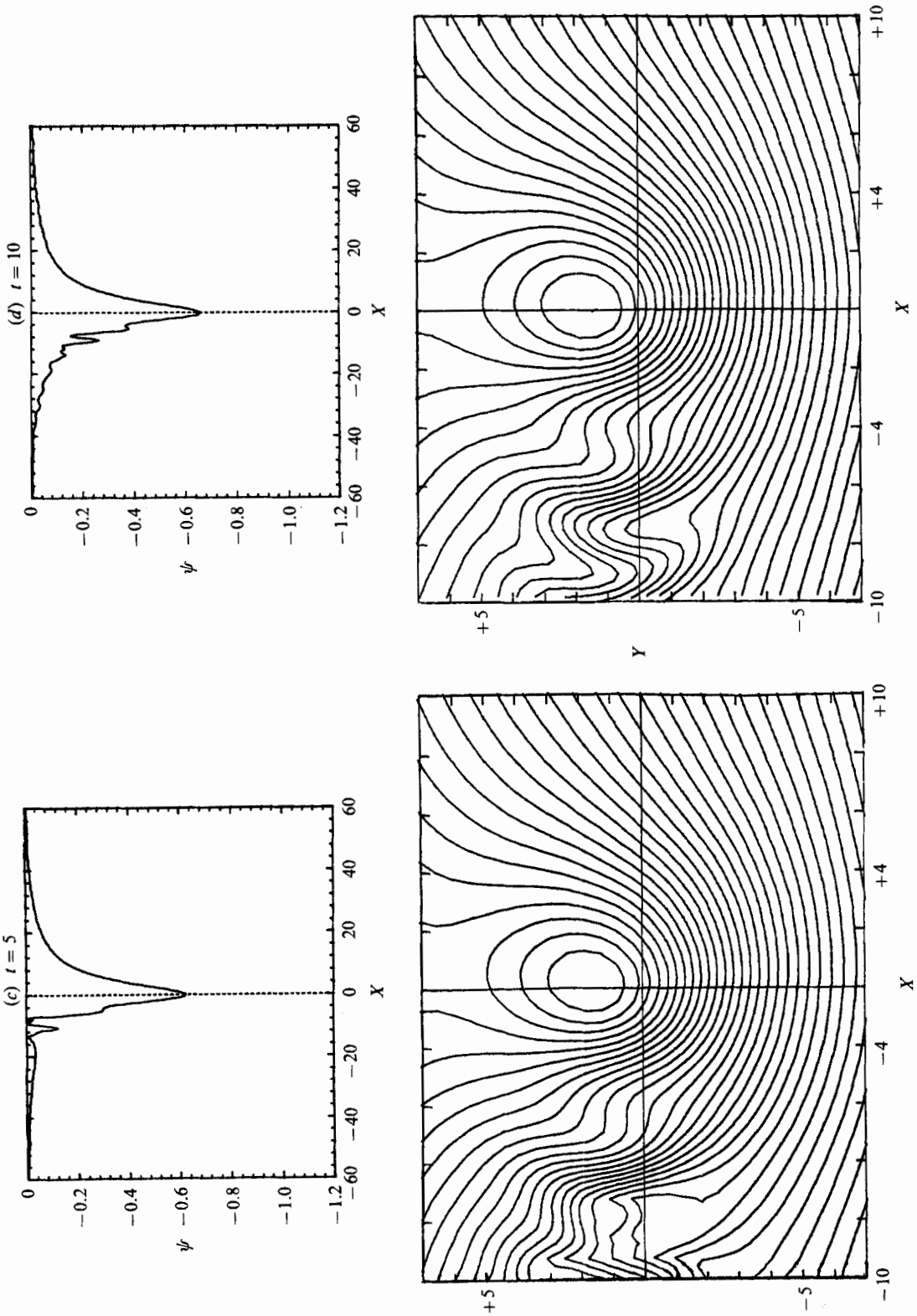

FIGURE 3 (*a–d*). For caption see next page.

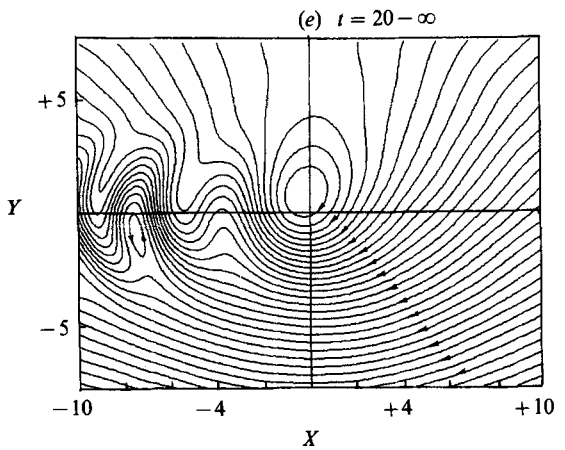

FIGURE 3. Normalized perturbation pressure ψ as a function of $X = x'/\hat{z}$ in the plane $Y = y/\hat{z} = 0.5$ (top), and corresponding horizontal (X, Y) streamline patterns (bottom), at a reduced height $\hat{z} = z/(2L/R) = 0.5$ above the three-dimensional topography $z_w^*/L = \tau(1+x'^2+y^2)^{-2}$ located in the centre, with a non-dimensional thickness ratio $\tau = 0.25$ and stratification parameters $\theta = 5$, at different times. (*a*) $t = 0.5$, (*b*) 1, (*c*) 5, (*d*) 10, (*e*) $20 = \infty$.

Each figure shows the distribution of the normalized perturbation pressure ψ as a function of $X = x'/\hat{z}$ in the plane $Y = y/\hat{z} = 0.25$, and the corresponding streamlines in the (X, Y)-plane. A region of high pressure (recall $\psi = -2p$) implies an anticyclonic disturbance, causing a clockwise twist of the streamlines.

During the early evolutionary stage of the solution, the anticyclonic motion builds up at $t = O(1)$ well before the familiar inertial-wave modes appear. This is to be expected in view of the wavenumber window established by the unit circular step function $\Pi(t-b)$ in the solution (3.3), (3.7), which begins with a zero width at time zero. Subsequently, various wave modes appear both upstream and downstream of the obstacle, but as time increases, consistent with the results for frequency response of Brown & Cheng (1987), most of the wavy modes disappear on the upstream side and move downstream. Finally, wavy features can be detected mainly on the downstream in the form of densely packed lee waves. In the meantime, the pressure hill associated with the large-scale anticyclonic motion first increases to a maximum then decreases to a local minimum before approaching the steady state. This, together with the growing inertial wave modes in the lee, gives the appearance (impression) of generation and shedding of a *secondary* (horizontal) eddy towards the final stages of the evolution. The solution eventually approaches steady state (equilibrium) in which a small-scale cyclonic eddy (opposite of the large-scale motion) appears in the lee of the obstacle.

It is essential to point out here that the equilibrium solution (figure 3*e*) is not identical to the steady-state solution presented in figure 6 of I; a difference in the stagnation point location at the north is apparent from the streamline patterns. The discrepancy results from a scaling error in the calculation of the total stream function (cf. (4.1) in I). The essential features brought out therein, concerning the main anticyclone and the cyclonic eddy, however, remain unchanged in figure 3(*e*).

The relatively early appearance of the cyclonic modes can be attributed to the

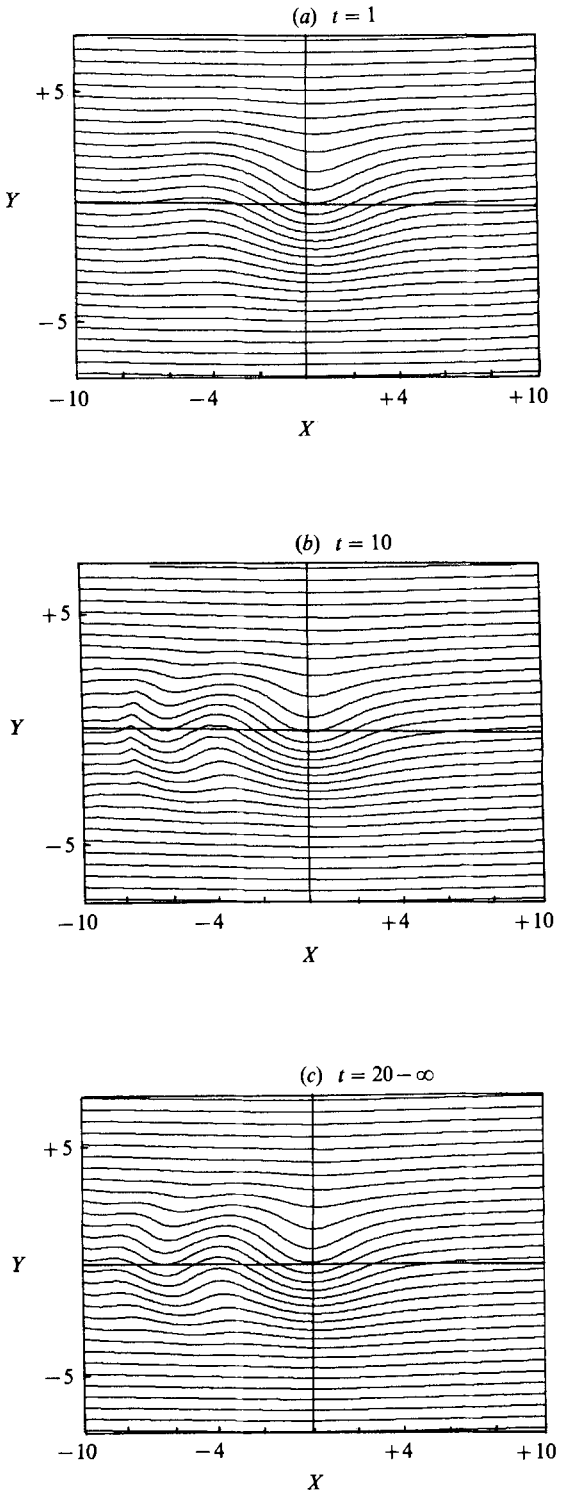

FIGURE 4. The same case as figure 3, but for $\theta = 1$, (*a*) $t = 1$, (*b*) 10, (*c*) 20–∞.

higher group velocities enjoyed by the long waves. The dispersion relation of (2.6*a*) for a wavetrain $\psi \sim e^{i(\omega x' + \sigma y + kz - \Omega t)}$ yields

$$\frac{\partial \Omega}{\partial \omega} : \frac{\partial \Omega}{\partial \sigma} : \frac{\partial \Omega}{\partial k} \sim \omega : \sigma : -1, \tag{4.2a}$$

$$\frac{\partial \Omega}{\partial k} \sim (\omega^2 + \sigma^2)^{-\frac{3}{2}} \gg 1 \tag{4.2b}$$

for vanishing ω and σ. Thus, the group velocities of the smooth, anticyclonic modes corresponding to vanishingly small ω and σ can evolve much earlier; in fact, according to (4.2) they will appear far above the obstacle, and directly overhead. Also note that the anticyclonic disturbance shown in figure 3(*a–e*) appears to be rather far north of the mountain and remains displaced for a long time. This may be correlated with the pressure-level overshoot (cf. figure 3*b*) at $t \approx 1$, which causes the stagnation point to move slightly northward, giving a greater degree of streamline-pattern asymmetry.

The possibility of disturbances propagating upstream of the obstacle during the evolution of the flow could also have been anticipated from the study by Redekopp (1975), based on group-velocity considerations, as discussed in Brown & Cheng (1987).

Associated with the anticyclone is a stagnation point at the far north ($Y \sim 5$–7) which may be inferred from the streamline contours as early as $t = 1$. This is not too surprising in view of the relatively large θ considered in this example and similar features found in Hogg's solution in the steady limit (valid for large θ even for a thickness ratio $\tau = O(\theta^{-\frac{1}{2}})$). Therefore the linear equations (2.6) for the pressure remain valid even in the regime $\tau\theta^{\frac{1}{2}} = O(1)$ (cf. I).

The cyclonic eddy appearing in the lee at large t is interesting, but lacks the full support of an asymptotic theory, since its occurrence requires the coexistence of the anticyclonic eddy and inertial waves, for which the adequacy of the linear PDE (2.6*a*, *b*) may be questioned. A close examination shows that the linearization leading to (2.6*a*, *b*) amounts to replacing the derivative $\mathrm{D}^2/\mathrm{D}t^2$ by $(\partial/\partial t - u_c\,\partial/\partial x)^2$ in the full equation, which is at least justifiable for the early periods. In any case, the example may be regarded as a transition model capable of reaching both the high and low stratification limits. The interesting features brought out by this transition model are certainly valuable in providing a focus for the more critical nonlinear analysis to follow.

Figure 4(*a–c*) presents the horizontal streamline pattern over the same topography and altitude but for a lower degree of stratification, $\theta = 1$. The velocity perturbations are considerably smaller in this case and there is no sign of closed streamlines.

Finally, as a point of potential interest to experimental detection of the high (low) pressure region and the related anticyclonic (cyclonic) motion, we examine the effects resulting from the difference in bottom geometry (for the same thickness ratio). Both studies for the steady and oscillating topographies (I and Brown & Cheng 1987, respectively) show that the anticyclonic (cyclonic) far field is determined mainly by the displacement *volume* of the topography. Although an asymptotic analysis has not been carried out for the present solution, similar dependence on the displacement volume is expected. In fact, it should have been obvious from the relation with the sinusoidally pulsating solution via the Duhamel integral discussed in §3.4. Corresponding effects due to noticeable differences in displacement volume are also expected in the near field, although the relationship is not so explicit. Thus

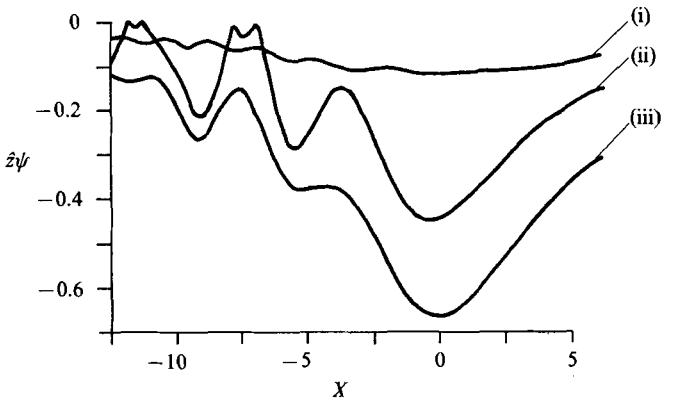

FIGURE 5. Normalized perturbation pressure $\hat{z}\psi$ as a function of X in the plane $Y = 0.5$ at $\hat{z} = 0.5$ for three different topographies: (i) spherical cap, (ii) truncated cylinder, and (iii) the smooth topography of figures 3 and 4. These three examples may be considered to have the same thickness ratio, but there displacement volumes are widely different.

consideration of the steady-state solutions will suffice for the purpose of showing the difference.

Figure 5 shows a rescaled perturbation pressure $\hat{z}\psi$ as a function of X at $\hat{z} = 0.5$ in the plane of symmetry for three different bottom geometries: (i) a spherical cap, (ii) a truncated cylinder and (iii) the smooth topography considered in the analyses presented in figures 3 and 4, all of which have the same thickness ratio of $\tau = 0.25$. In spite of the equal thickness, the displacement volumes of the three geometries (i), (ii) and (iii) are in the proportion 1:2:4, respectively. Figure 5 confirms the anticipated significant differences among the three examples, while a good correlation of the three results through the far-field formulas is not possible since $\hat{z} = 0.5$ is not large enough. In fact, the relative pressure level over the spherical cap is seen to be considerably lower than expected from the far-field analysis.

5. Summary and concluding remarks

Earlier work, I, showed that the steady-state relative motion of an obstacle at the horizontal base of a stably stratified deep rotating fluid supports not only lee waves at great (scaled) heights, but also a high (low)-pressure region associated with an anticyclonic (cyclonic) disturbance in the far field, which depends mainly on the obstacle displacement volume. Except in the homogeneous limit ($\theta = 0$), this feature exists at all degrees of stratification. In the linearized framework, the present evolution analysis confirms that this steady-state feature is unique, and realizable at the end of an evolutionary process ($t \to \infty$). An explicit analytical solution for the indicial response, that is the case of impulsive acceleration of the obstacle to a uniform speed, is obtained and indicates that, at any given time, only the wavenumbers in a wavenumber window contribute to the solution. The radius of this wavenumber window is zero at the beginning and increase linearly with time. Consistent with this description, a solution computed via an FFT algorithm for a three-dimensional topography reveals that a relatively large-scale anticyclonic (cyclonic) disturbance generated by an obstacle associated with the lowest wavenumber $\omega = \sigma = 0$ appears very early in the evolutionary process. As time increases, with the increase in the radius of the wavenumber window, other higher

wavenumbers can appear upstream as well as downstream of the topography. Eventually most of the upstream wave modes disappear or move downstream and the solution approaches its steady-state limit. The rapid build-up and persistence of the anticyclonic (cyclonic) disturbance along with the subsequent growth of the inertial waves in the lee results in what appears to be a generation process of a secondary horizontal eddy of the opposite sense at the final stage of the evolution.

In the recent work of Brown & Cheng (1987) on pulsating topography, detailed far-field analyses indicate that flow-field features can differ widely depending on whether the forcing frequency Ω exceeds a frequency threshold given by the Brunt–Väisälä value N. Our numerical solution shows that waves are present ahead of the topography mainly in an earlier period corresponding to the supercritical case ($\Omega > N$), and confirming therefore the feature associated with the threshold frequency. The response of the flow to these two different types (the indicial and sinusoidal pulsating) of the obstacle motion presents two complementary descriptions of the time-dependent problem.

Studies by Richardson (1980), Reitan (1974), and others have indicated the topographical origin of some of the large eddies observed near seamounts, as well as the generation of smaller-scale cyclones in the lee of major mountain ranges. The Tibetan highland, for example, is believed to have a far-reaching influence on the weather in Asia, particularly as a major cause for the zonal-wind deflection southward over the Indian and Pacific oceans, contributing to the high humidity over the east China coast in late spring and the monsoon in south-east Asia during the summer. Laboratory studies of Chen (1982) substantiate the belief that the topography and the Coriolis acceleration, rather than the β-effect, are the major contributing factors, Chen's conclusion appears to be in general accord with the cyclonic features brought out here and in I, although our assumption of a vanishing Rossby number will not allow a quantitative comparison. Detailed comparison of the field observations with related theoretical works have also proven problematical (see Smith 1979*c*) and Richardson 1980 for several examples). This may be partially due to the fact that conditions surrounding the phenomena in nature, such as the shape of the topography, stratification, etc., are more complex than the simplified model stipulated in theoretical works.

It must be emphasized once again that the present theory cannot predict very accurately events in the atmosphere and ocean, because the parameter $\theta = (N/\Omega_c)^2/R^2$ is taken as a unit-order quantity in the formal analysis. Since R is assumed to be small, N/Ω_c has to be quite small for a unit-order θ; this is not the case in atmosphere and may be valid only in special circumstances in the ocean. The objective of our analysis, however, has been aimed at understanding the approach to equilibrium, and in providing a transition model capable of reaching both the high and the low stratification limits. Furthermore, this model suggests that the emergence of a small-scale eddy in the lee is feasible at least in an experimental set-up where the inertial waves and the anticyclonic eddy can be made to coexist.

While analysis such as the present work bring out some of the fundamental features of these problems, more thorough theoretical and experimental work is needed to provide a better understanding of the actual flows in the oceans and atmosphere. More specifically, the effects of finite Rossby number in controlling the early evolution stage and the very important nonlinear analysis should be addressed.

How the viscous contributions, including Ekman pumping, may alter the lee-wave patterns (and the secondary eddies) represent another area of importance. Obviously, the formation of the secondary cyclonic eddies must be critically examined in a

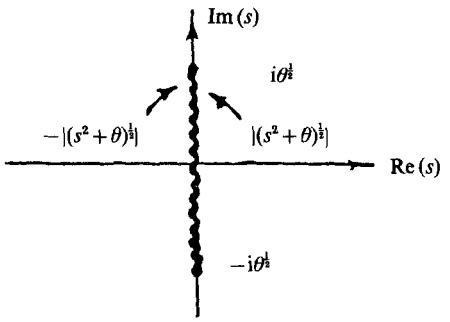

FIGURE 6. Definition of $(s^2+\theta)^{\frac{1}{2}}$ in the complex $-s$ plane.

nonlinear analysis. There is still an unanswered question as to whether the phenomenon of blocking or the layer-independence principle familiar in the stratified-flow theory (Yih 1965; Pierrehumbert 1987) can be recovered in some proper limit from the linearized framework adopted here.

Finally, changes brought about by various shapes of the three-dimensional topography are of interest, particularly to experimental investigations for the detection of features brought out in the foregoing analysis. Examples studied in figure 5 confirm the strong dependence of the anticyclonic feature on the displacement volume, rather than the thickness ratio, of the topography, which could be easily overlooked in a corresponding laboratory study.

This research was supported by the US National Science Foundation, Engineering Division through Grant MEA-8217833 to the University of Southern California. We would like to thank Professors S. N. Brown and L. G. Redekopp for helpful discussions.

Appendix

We would like to show that for $b \geqslant 0$

$$\mathscr{L}^{-1}\frac{i\omega(s-i\omega)-\theta}{s[(s-(\omega)^2+\theta)]^{\frac{1}{2}}}\exp\{-b[(s-i\omega)^2+\theta]^{\frac{1}{2}}\} = \left\{i\omega\,e^{i\omega t}J_0[\theta(t^2-b^2)]^{\frac{1}{2}}+(\omega^2-\theta)\int_b^t e^{i\omega p}J_0[\theta(p^2-b^2)]^{\frac{1}{2}}dp\right\}\Pi(t-b), \quad (A\,1)$$

where J_0 is the Bessel function of the first kind zeroth order, the function $\Pi(t-b)$ is defined as

$$\Pi(t-b)=\begin{cases}1, & t>b,\\ 0, & t\leqslant b,\end{cases}$$

and $\mathscr{L}^{-1}$ signifies the inverse Laplace transform operator. We start with the following inversion formula. For $b \geqslant 0$

$$\mathscr{L}^{-1}\left\{\frac{1}{(s^2+\theta)^{\frac{1}{2}}}\exp[-b(s^2+\theta)^{\frac{1}{2}}]\right\} = J_0[\theta(t^2-b^2)]^{\frac{1}{2}}\Pi(t-b).$$

The proof of this inversion can be found in Parodi (1957). Essential to this proof is the proper choice of the branch cut and the definition of the function $(s^2+\theta)^{\frac{1}{2}}$ in the complex-s plane shown in figure 6.

The left-hand side of (A 1) now can be written as

$$i\omega\mathscr{L}^{-1}\frac{1}{[(s-i\omega)^2+\theta]^{\frac{1}{2}}}\exp\{-b[(s-i\omega)^2+\theta]^{\frac{1}{2}}\}$$
$$+(\omega^2-\theta)\,\mathscr{L}^{-1}\frac{1}{s[(s-i\omega)^2+\theta]^{\frac{1}{2}}}\exp\{-b[(s-i\omega)^2+\theta]^{\frac{1}{2}}\}$$

using the shifting theorem and the derivative rule (A 1) can now readily be shown.

REFERENCES

Batchelor, G. K. 1967 *An Introduction to Fluid Dynamics*. Cambridge University Press.

Brown, S. N. & Cheng, H. K. 1987 *J. Fluid Mech.* **171**, 359.

Buzzi, A. & Tibaldi, S. 1977 *Q. J. R. Met. Soc.* **103**, 135.

Chen, R. 1982 *Scientia Sinica* **27**, 184.

Cheng, H. K. 1977 *Z. Angew Math. Phys.* **28**, 753.

Cheng, H. K., Hefazi, H. & Brown, S. N. 1984 *J. Fluid Mech.* **141**, 431.

Cheng, H. K. & Johnson, E. R. 1982 *Proc. R. Soc. Lond.* A **383**, 71.

Chung, Y. S., Hage, K. D. & Reinelt, E. R. 1976 *Mon. Weather Rev.* **104**, 879.

Egger, J. 1974 *Mon. Weather Rev.* **102**, 847.

Hefazi, H. 1985 Ph.D. Thesis, University of Southern California.

Hide, R. 1971 *J. Fluid Mech.* **49**, 745.

Hide, R., Ibbetson, A. & Lighthill, M. J. 1968 *J. Fluid Mech.* **32**, 251.

Hogg, N. G. 1973 *J. Fluid Mech.* **58**, 517.

Hogg, N. G. 1980 Effect of bottom topography on ocean currents. In *Orographic Effects in Planetary Flows*; GARP Publ. Series, vol. 23, p. 169.

Huppert, H. E. 1975 *J. Fluid Mech.* **67**, 397.

Huppert, H. E. & Bryan, K. 1975 *Deep-Sea Res.* **23**, 655.

Ingersoll, A. P. 1969 *J. Atmos. Sci.* **26**, 744.

Lighthill, M. J. 1965 *J. Inst. Maths Applics* **1**, 1.

Lighthill, M. J. 1967 *J. Fluid Mech.* **27**, 725.

Lighthill, M. J. 1978 *Waves in Fluids*. Cambridge University Press.

Manabe, S. & Terpstra, T. B. 1974 *J. Atmos. Sci.* **31**, 3.

Parodi, M. 1957 *Introduction A L'etude L'analyse Symbolique*. Paris: Imprimeur-Libraire.

Pedlosky, J. 1979 *Geophysical Fluid Dynamics*. Springer.

Pierrehumbert, R. T. 1987 *Mesocale Analysis Forecasting*, pp. 493–575. American Meteorological Society.

Queney, P. 1948 *Bull. Am. Met. Soc.* **29**, 16.

Redekopp, L. G. 1975 *Geophys. Fluid Dyn.* **6**, 289.

Reitan, C. H. 1974 *Mon. Weather Rev.* **102**, 861.

Richardson, P. L. 1980 *J. Mar. Res.* **28**, 673.

Smith, R. 1979*a* *J. Atmos Sci.* **36**, 177.

Smith, R. 1979*b* *J. Atmos. Sci.* **36**, 2395.

Smith, R. 1979*c* *Adv. Geophys.* **21**, 87.

Whitham, G. B. 1973 *Linear and Nonlinear Waves*. Wiley.

Yih, C. S. 1965 *Dynamics of Nonhomogeneous Fluids*. Macmillan.

Yih, C. S. 1980 *Stratified Flows*. Academic.